Sports Medicine and Health Science 8 (2026) 110–118

Contents lists available at ScienceDirect

Sports Medicine and Health Science

journal homepage: www.keaipublishing.com/smhs

Commentary

An exerkine-based prognostic index reveals immune heterogeneity and predicts outcomes across 33 cancers

ARTICLE INFO

Keywords
Exerkines
Exercise oncology
Cancer prognosis
Tumor microenvironment
Immune checkpoint
Machine learning

ABSTRACT

Background: Exercise exerts tumor-suppressive effects across multiple malignancies, partly through exerkines—exercise-induced secreted factors with immunomodulatory and metabolic functions. However, the prognostic relevance of exerkines across cancer types remains unclear, and the molecular determinants of exercise responsiveness are poorly defined.

Methods: We systematically profiled 183 curated exerkine-related genes across 33 cancer types from The Cancer Genome Atlas (TCGA) using non-negative matrix factorization (NMF) to define molecular subtypes. Prognostic significance was evaluated via Kaplan-Meier analysis. For five cancers with consistent survival divergence (LGG, KIRC, LUAD, PAAD, ACC), we developed an Exerkine Prognostic Index (EPI) using LASSO Cox regression and validated its predictive performance through time-dependent ROC analysis. Immune cell infiltration (CIBERSORT), stromal/immune scores (ESTIMATE), and immune checkpoint expression were assessed to characterize immune landscape differences between EPI subgroups.

Results: Exerkine-based NMF clustering identified prognostically distinct subtypes in 25 cancers. The EPI robustly stratified patients into high- and low-risk groups with significant differences in overall survival ($p < 0.001$). High-EPI subgroups were associated with elevated infiltration of immunosuppressive cells (e.g., Tregs, M0 macrophages), altered immune/stromal scores, and differential expression of immune checkpoints such as PD-L1 and CTLA4 in a cancer-type-specific manner.

Discussion: Our findings reveal that exerkine expression patterns capture biologically and clinically relevant heterogeneity across cancers. The EPI provides a robust molecular tool to stratify patients by prognosis and immune contexture, offering insights into differential exercise responsiveness.

Conclusions: Exerkines represent promising biomarkers for risk stratification and precision-guided exercise interventions in oncology.

1. Introduction

Accumulating evidence underscores exercise as a multifaceted adjunctive strategy in oncology, capable of attenuating tumorigenesis, enhancing therapeutic efficacy, and improving quality of life in cancer patients. Major clinical organizations—including the American College of Sports Medicine (ACSM), American Cancer Society (ACS), and American Society of Clinical Oncology (ASCO)—now endorse structured exercise regimens as integral to cancer care guidelines, reflecting its systemic benefits across treatment and survivorship settings.[1–3] Mechanistically, exercise modulates tumor biology through pleiotropic pathways: it enhances immunosurveillance by mobilizing cytotoxic lymphocytes and natural killer cells, reprograms metabolic crosstalk within the tumor microenvironment (TME) via lactate shuttling and oxidative stress regulation, and normalizes aberrant tumor vasculature, thereby facilitating drug delivery and sensitizing tumors to therap.[4]

However, the therapeutic potential of exercise remains variably expressed across malignancies, owing to profound intertumoral heterogeneity. Similar to pharmacologic interventions, exercise-induced effects are context-dependent and influenced by tumor-intrinsic features such as molecular subtype, mutational burden, stromal infiltration, and immunogenicity.[5] For instance, while exercise-induced IL-6 can stimulate anti-inflammatory cytokine production and reduce cancer cell proliferation/DNA damage, it may activate tumour-intrinsic signalling pathways and regulate pro-tumour behaviour in infiltrating stromal/immune cells.[6] These paradoxical responses highlight the pressing need for biomarkers that can predict exercise responsiveness in a cancer-type-specific manner.

A promising molecular interface linking exercise to cancer biology lies in exerkines—a class of bioactive molecules secreted by skeletal muscle, adipose tissue, liver, and other organs in response to physical activity. These include myokines (e.g., irisin, IL-15), adipokines (e.g., leptin, adiponectin), and hepatokines (e.g., FGF21), which exert systemic effects on metabolism, inflammation, and immunity.[7] Certain exerkines such as SPARC and oncostatin M exhibit antitumor properties by inhibiting angiogenesis and remodeling the immunosuppressive TME, whereas others like IL-6 demonstrate dual roles depending on tumor type, concentration, and local context.[6,8] Yet, their pan-cancer relevance as prognostic or therapeutic biomarkers remains largely unexplored.

Peer review under the responsibility of Editorial Board of Sports Medicine and Health Science

https://doi.org/10.1016/j.smhs.2025.05.002
Received 19 December 2024; Received in revised form 12 April 2025; Accepted 17 May 2025
Available online 20 May 2025

Abbreviations

ACSM	American College of Sports Medicine
ACS	American Cancer Society
ASCO	American Society of Clinical Oncology
TME	Tumor microenvironment
TCGA	The Cancer Genome Atlas
NMF	Non-negative matrix factorization
EPI	Exerkine Prognostic Index
ACC	Adrenocortical carcinoma
BLCA	Bladder urothelial carcinoma
BRCA	Breast invasive carcinoma
CESC	Cervical squamous cell carcinoma and endocervical adenocarcinoma
CHOL	Cholangiocarcinoma
COAD	Colon adenocarcinoma
DLBC	Diffuse large B-cell lymphoma
ESCA	Esophageal carcinoma
GBM	Glioblastoma multiforme
HNSC	Head and neck squamous cell carcinoma
KICH	Kidney chromophobe
KIRC	Kidney renal clear cell carcinoma
KIRP	Kidney renal papillary cell carcinoma
LAML	Acute myeloid leukemia
LGG	Brain lower grade glioma
LIHC	Liver hepatocellular carcinoma
LUAD	Lung adenocarcinoma
LUSC:	Lung squamous cell carcinoma
MESO	Mesothelioma
OV	Ovarian serous cystadenocarcinoma
PAAD	Pancreatic adenocarcinoma
PCPG	Pheochromocytoma and paraganglioma
PRAD	Prostate adenocarcinoma
READ	Rectum adenocarcinoma
SARC	Sarcoma
SKCM	Skin cutaneous melanoma
STAD	Stomach adenocarcinoma
TGCT	Testicular germ cell tumors
THCA	Thyroid carcinoma
THYM	Thymoma
UCEC	Uterine corpus endometrial carcinoma
UCS	Uterine carcinosarcoma
UVM	Uveal melanoma
DEGs	Differentially expressed genes

In this study, we hypothesize that exerkine expression profiles stratify tumors into exercise-responsive and -refractory subtypes, thereby offering a molecular basis for personalized exercise oncology. Leveraging multi-omics datasets from The Cancer Genome Atlas (TCGA), we performed non-negative matrix factorization (NMF) to define exerkine-driven molecular subtypes across 33 cancer types, systematically evaluated their prognostic significance, and constructed a machine learning-based Exerkine Prognostic Index (EPI) to predict risk and immune phenotypes. Our findings aim to resolve the "exercise-oncology paradox" by illuminating the molecular heterogeneity underlying exercise efficacy and to lay the groundwork for precision-guided exercise interventions in oncology.

2. Materials and methods

2.1. Data acquisition and processing

We analyzed transcriptomic and clinical data across 33 cancer types from The Cancer Genome Atlas (TCGA), including Adrenocortical carcinoma (ACC, $n = 81$), Bladder urothelial carcinoma (BLCA, $n = 411$), Breast invasive carcinoma (BRCA, $n = 1\,098$), Cervical squamous cell carcinoma and endocervical adenocarcinoma (CESC, $n = 306$), Cholangiocarcinoma (CHOL, $n = 45$), Colon adenocarcinoma (COAD, $n = 376$), Diffuse large B-cell lymphoma (DLBC, $n = 50$), Esophageal carcinoma (ESCA, $n = 198$), Glioblastoma multiforme (GBM, $n = 176$), Head and neck squamous cell carcinoma (HNSC, $n = 520$), Kidney chromophobe (KICH, $n = 93$), Kidney renal clear cell carcinoma (KIRC, $n = 534$), Kidney renal papillary cell carcinoma (KIRP, $n = 325$), Acute myeloid leukemia (LAML, $n = 175$), Brain lower grade glioma (LGG, $n = 536$), Liver hepatocellular carcinoma (LIHC, $n = 359$), Lung adenocarcinoma (LUAD, $n = 508$), Lung squamous cell carcinoma (LUSC, $n = 495$), Mesothelioma (MESO, $n = 89$), Ovarian serous cystadenocarcinoma (OV, $n = 311$), Pancreatic adenocarcinoma (PAAD, $n = 179$), Pheochromocytoma and paraganglioma (PCPG, $n = 189$), Prostate adenocarcinoma (PRAD, $n = 498$), Rectum adenocarcinoma (READ, $n = 107$), Sarcoma (SARC, $n = 267$), Skin cutaneous melanoma (SKCM, $n = 463$), Stomach adenocarcinoma (STAD, $n = 407$), Testicular germ cell tumors (TGCT, $n = 158$), Thyroid carcinoma (THCA, $n = 509$), Thymoma (THYM, $n = 124$), Uterine corpus endometrial carcinoma (UCEC, $n = 203$), Uterine carcinosarcoma (UCS, $n = 59$), and Uveal melanoma (UVM, $n = 82$). Raw RNA-sequencing data and corresponding clinical annotations were retrieved from the TCGA database (https://cancergenome.nih.gov/). All datasets were uniformly preprocessed using TCGA-standardized normalization and quality control pipelines to ensure cross-cancer comparability. Normal tissue samples were excluded to focus exclusively on tumor-specific molecular profiles.

2.2. NMF-based consensus clustering for molecular subtyping

Consensus clustering was performed using non-negative matrix factorization (NMF) with the Brunet algorithm, implemented via the "NMF" R package. Analyses were restricted to 31 previously reported exercise-induced secreted factors (exerkines), including ADIPOQ, ANGPT1, ANGPTL4, APLN, BDNF, CTSB, AHSG, CX3CL1, FGF21, FST, GDF15, GPLD1, HSPA1A, IL1RN, IL6, IL7, CXCL8, IL10, IL13, IL15, FNDC5, LIF, METRNL, CTRP15, OSTN, MSTN, SPARC, SDC4, TGFB1, TGFB2, and VEGFA.[7] Genes with undetectable expression (TPM = 0) in $\geq$ 50% of samples were excluded to reduce technical noise. Cluster robustness was evaluated via 1 000 subsampling iterations. Kaplan-Meier survival analysis (log-rank test; "survival" R package v3.7-0) was used to evaluate prognostic significance, with $p < 0.05$ considered statistically significant.

2.3. Development of the exerkine prognostic index (EPI)

To construct a robust prognostic model, we focused on five cancers (LGG, KIRC, LUAD, PAAD, ACC) that showed the most significant survival differences between NMF-defined clusters. Binary classification ($k = 2$) was adopted to minimize class imbalance and improve model generalizability. Differentially expressed genes (DEGs) were identified using DESeq2 (v1.44.0) with thresholds of $p < 0.05$ and $|\log_2(\text{FoldChange})| > 1$. Prognosis-associated genes were then filtered via univariate Cox regression, followed by LASSO regression with 10-fold cross-validation to avoid overfitting. The Exerkine Prognostic Index (EPI) was constructed using the formula:

$$\text{EPI} = \sum(\text{Coef}i \times \text{Expr}i)$$

where Coefi is the LASSO-derived coefficient and Expri is the $\log_2(\text{TPM} + 1)$-transformed expression value of each selected gene. Optimal cutoff values for EPI-based risk stratification were determined using maximally selected rank statistics (R package "survminer" v0.4.9). Prognostic performance was validated through Kaplan-Meier and time-dependent ROC analyses.

2.4. Immune landscape and tumor microenvironment assessment

Immune infiltration across high- and low-EPI subgroups was estimated using CIBERSORT (v0.1.0; LM22 signature) to deconvolute 22 immune cell types. The ESTIMATE algorithm was used to compute ImmuneScore, StromalScore, and ESTIMATEScore, providing insight into tumor purity and microenvironment composition. Comparisons between risk groups were conducted to assess immune heterogeneity.

2.5. Statistical analysis

All statistical analyses were conducted in R (v4.4.1). Group comparisons were performed using Mann-Whitney *U* tests for non-parametric data or Student's *t*-tests for parametric data. Significance was set at $p < 0.05$. Statistical annotations were denoted as follows: ns (not significant, $p \geq 0.05$), * ($p < 0.05$), ** ($p < 0.01$), *** ($p < 0.001$), and **** ($p < 0.000\ 1$).

3. Results

3.1. Exerkine-driven molecular subtypes reveal prognostic heterogeneity across malignancies

Non-negative matrix factorization (NMF) clustering of exerkine expression profiles within the TCGA cohort stratified patients into distinct molecular subtypes, with the number of clusters (k) ranging from 2 to 10 per cancer type. Optimal k-values were selected based on both survival significance and sample size constraints to avoid overfitting (Fig. 1). Survival analysis using Kaplan-Meier curves demonstrated significant prognostic divergence (log-rank $p < 0.05$) in 25 out of 33 malignancies, including LGG, KIRC, LUAD, PAAD, ACC, KIRP, MESO, UVM, LAML, UCEC, CESC, COAD, STAD, LIHC, THYM, BLCA, BRCA, LUSC, PCPG, CHOL, HNSC, KICH, PRAD, THCA, and UCS (Fig. 2).

Across cluster configurations (k = 2–10), over three-quarters of cancer types exhibited at least one high-risk subgroup associated with significantly worse overall survival, supporting the prognostic relevance of exerkine-derived subtyping (Fig. 3). Notably, LGG, KIRC, LUAD, PAAD, and ACC consistently harbored high-risk clusters across nearly all tested cluster granularities, suggesting that exerkines may serve as tumor-context-dependent biomarkers of outcome. These findings highlight the potential of exerkine-driven molecular stratification in identifying clinically meaningful subtypes across a wide spectrum of malignancies.

3.2. Machine learning-driven prognostic index construction and multi-cohort validation

To construct a robust and interpretable prognostic model, we focused on five cancers (LGG, KIRC, LUAD, PAAD, ACC) with the most pronounced and consistent survival stratification across NMF-derived clusters. For model development, we applied binary clustering ($k = 2$) to balance subtype separation with statistical power. Differential expression analysis between high- and low-risk NMF subgroups identified 4 627, 3 295, 2 644, 4 709, and 5 003 significantly altered genes in LGG, KIRC, LUAD, PAAD, and ACC, respectively (Fig. 4A–E).

Univariate Cox regression pinpointed thousands of survival-associated genes per cancer type (Table S1), which were then subjected to LASSO regression with 10-fold cross-validation to generate the Exerkine Prognostic Index (EPI) (Fig. 4F–J). The EPI robustly stratified patients into high- and low-risk subgroups, with significantly worse overall survival observed in high-EPI groups across all five cancers (log-rank $p < 0.000\ 1$; Fig. 4K–O).

Time-dependent ROC analysis showed excellent prognostic performance, with 1-, 3-, and 5-year AUC values consistently exceeding 0.80 in LGG, LUAD, PAAD, and ACC, and surpassing 0.74 in KIRC (Fig. 4P–T). Alluvial plots revealed strong concordance between EPI-defined risk subgroups and NMF clusters: in LGG, KIRC, and PAAD, Cluster 2 predominantly aligned with the high-EPI group and poor prognosis, while in LUAD and ACC, high-risk features were enriched in Cluster 1 (Fig. 4U–Y). These results support the biological coherence of the EPI framework and its consistency with unsupervised molecular stratification.

3.3. Immune infiltration and checkpoint dysregulation across EPI-defined subgroups

To investigate the immunological landscape associated with exerkine-based risk stratification, we performed CIBERSORT and ESTIMATE analyses across high- and low-EPI groups in the five selected cancers. Notably, LGG tumors with high EPI scores exhibited a complex immune profile characterized by concurrent enrichment of immunosuppressive and cytotoxic components, including elevated proportions of M1 and M2 macrophages, $CD8^+$ T cells, neutrophils, follicular helper T cells, and regulatory T cells, alongside a marked depletion of memory B cells, monocytes, and $CD4^+$ T cell subsets. This suggests a paradoxical immune milieu of heightened activation and exhaustion.

In KIRC, the high-EPI group showed prominent infiltration of macrophages M0, plasma cells, activated $CD4^+$ memory T cells, and Tregs, while exhibiting reductions in resting dendritic cells, macrophages M2, monocytes, and NK cells. This pattern indicates a myeloid-dominated but functionally dysregulated immune context. LUAD tumors in the high-EPI subgroup similarly displayed dominant M0 and M1 macrophage infiltration and activated $CD4^+$ memory T cells, but with concomitant suppression of monocytes, dendritic cells, and B cells naive.

PAAD samples with high EPI scores revealed selective immune evasion mechanisms, with increased resting NK cells but reduced monocytes and activated NK cells, reflecting compromised innate immune surveillance. ACC high-risk tumors were uniquely marked by dendritic cell activation and eosinophil infiltration, coupled with suppression of M2 macrophages, resting mast cells, and activated NK cells.

ESTIMATE analysis further supported these immunological distinctions: high-EPI subgroups in LGG and KIRC exhibited significantly elevated StromalScore, ImmuneScore, and ESTIMATEScore, indicative of an immunologically active yet potentially suppressive microenvironment. In contrast, LUAD and ACC high-EPI groups demonstrated global reductions across all three scores, suggestive of immune-cold or desert-like niches. PAAD high-risk tumors showed a selective reduction in ImmuneScore without significant stromal changes, reflecting an intermediate immune phenotype (Fig. 5B).

Checkpoint analysis revealed tumor-specific expression shifts. PD-L1 was significantly upregulated in high-EPI groups of LUAD and ACC, but downregulated in KIRC, with no significant change in LGG and PAAD. CTLA4 expression increased significantly in high-EPI KIRC and LUAD, while remaining stable in LGG, PAAD, and ACC (Fig. 5C). These data suggest that checkpoint vulnerability may vary across exerkine-defined risk strata, potentially informing immunotherapy selection.

4. Discussion

This study systematically evaluated the prognostic potential of exerkine-based molecular subtyping across a pan-cancer landscape, highlighting significant heterogeneity in survival outcomes associated with exerkine expression patterns. Through NMF clustering, we uncovered high-risk molecular subtypes in over 75% of cancers examined, with consistent stratification power observed in LGG, KIRC, LUAD, PAAD, and ACC. These results suggest that exerkines may not only reflect intrinsic tumor biology but also participate in cancer progression through mechanisms that vary across tissue contexts.

To refine the prognostic utility of exerkines and enable individual-level risk prediction, we further constructed the Exerkine Prognostic Index (EPI) using machine learning algorithms across five representative cancers. The EPI model demonstrated robust stratification capability,

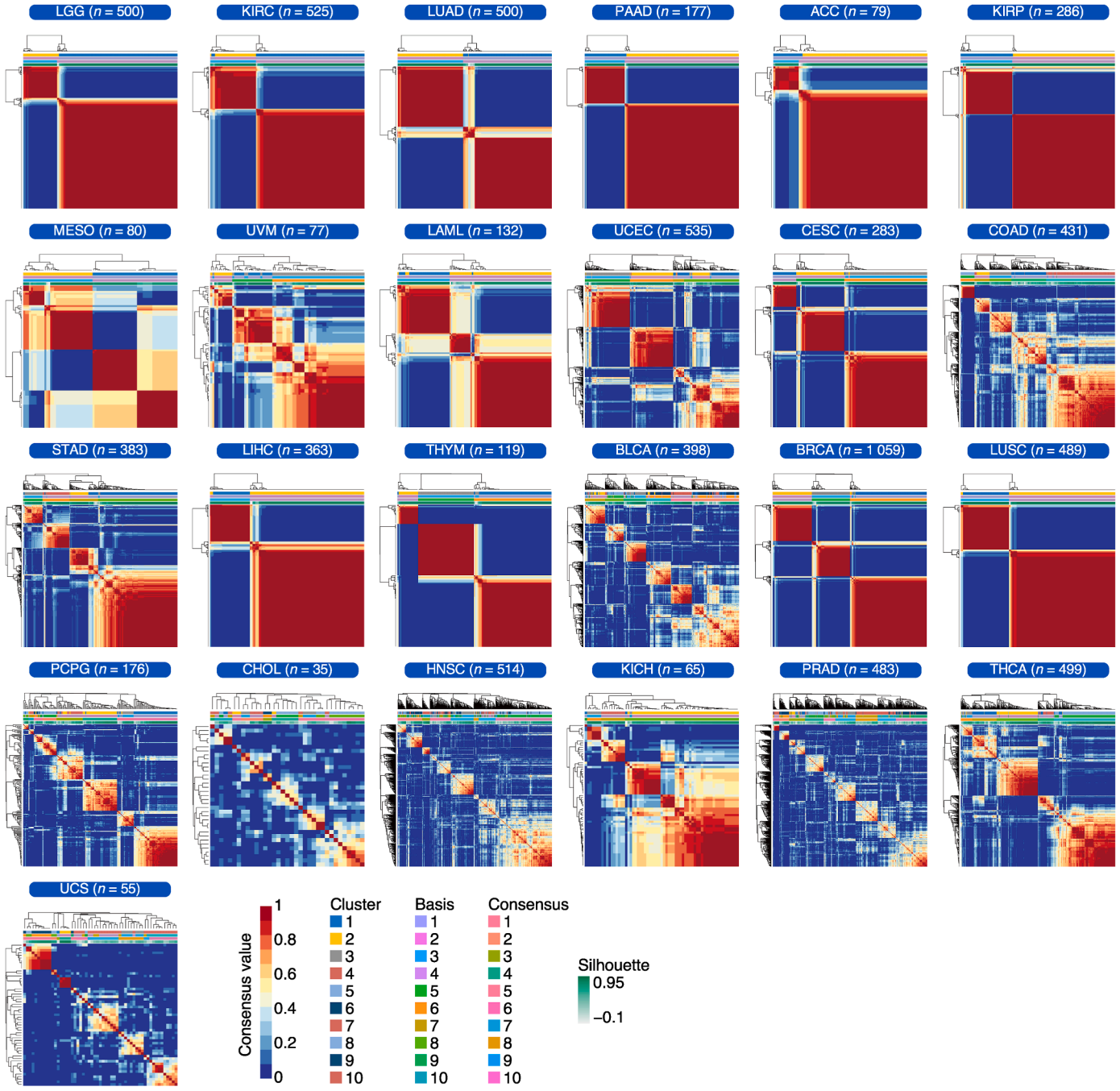

Fig. 1. Identification of exerkine-associated molecular subtypes via NMF clustering.
Consensus clustering matrices derived from non-negative matrix factorization (NMF) across 33 TCGA cancers using cluster numbers $k = 2$ to $k = 10$. Optimal k-values were selected based on prognostic significance (log-rank $p < 0.05$) and cohort size adequacy to mitigate overfitting. Only one representative clustering result per cancer is shown for clarity.
LGG: Brain Lower Grade Glioma; KIRC: Kidney renal clear cell carcinoma; LUAD: Lung adenocarcinoma; PAAD: Pancreatic adenocarcinoma; ACC: Adrenocortical carcinoma; KIRP: Kidney renal papillary cell carcinoma; MESO: Mesothelioma; UVM: Uveal melanoma; LAML: Acute myeloid leukemia; UCEC: Uterine corpus endometrial carcinoma; CESC: Cervical squamous cell carcinoma and endocervical adenocarcinoma; COAD: Colon adenocarcinoma; STAD: Stomach adenocarcinoma; LIHC: Liver hepatocellular carcinoma; THYM: Thymoma; BLCA: Bladder urothelial carcinoma; BRCA: Breast invasive carcinoma; LUSC: Lung squamous cell carcinoma; PCPG: Pheochromocytoma and paraganglioma; CHOL: Cholangiocarcinoma; HNSC: Head and neck squamous cell carcinoma; KICH: Kidney chromophobe; PRAD: Prostate adenocarcinoma; THCA: Thyroid carcinoma; UCS: Uterine carcinosarcoma.

with high-risk groups exhibiting significantly shorter overall survival. Importantly, the alignment between NMF-based clustering and EPI-defined risk subgroups suggests that exerkine-driven transcriptional programs are consistent and biologically coherent. Time-dependent ROC analysis validated the predictive performance of the EPI model, with AUC values exceeding 0.80 in most cancers, further supporting its clinical translation potential.

In-depth immune deconvolution and tumor microenvironment analyses provided further mechanistic insight into the clinical relevance of the Exerkine Prognostic Index (EPI). High-EPI subgroups demonstrated distinct immunological alterations that extended beyond generalized immune suppression. For instance, the high-EPI LGG subgroup exhibited

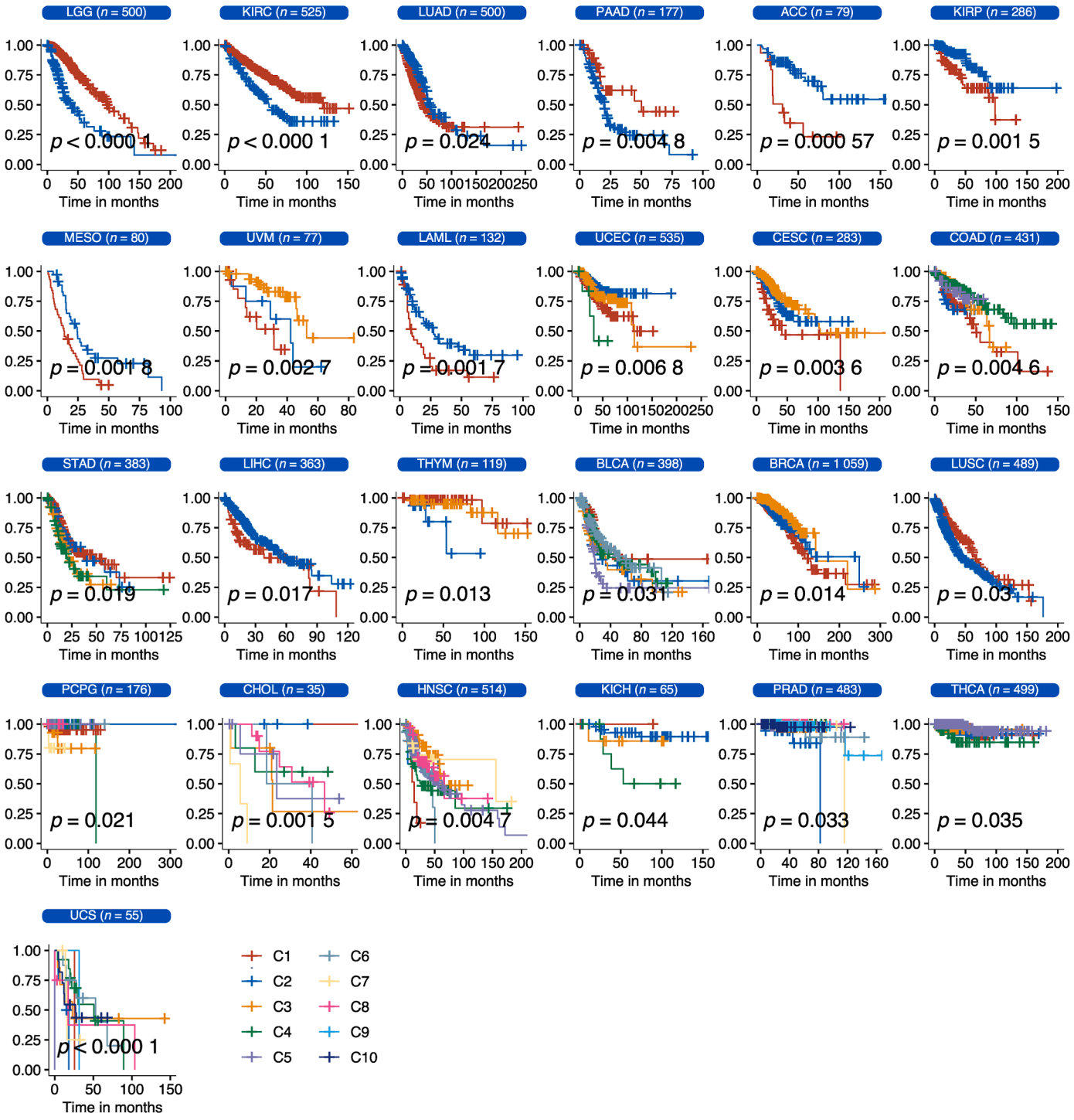

Fig. 2. Prognostic divergence among exerkine-derived molecular subtypes. Kaplan–Meier survival curves depicting overall survival differences among NMF-defined molecular subtypes in cancers with significant survival stratification (log-rank $p < 0.05$). Cluster configurations correspond to the optimal k-values selected in Fig. 1. LGG: Brain Lower Grade Glioma; KIRC: Kidney renal clear cell carcinoma; LUAD: Lung adenocarcinoma; PAAD: Pancreatic adenocarcinoma; ACC: Adrenocortical carcinoma; KIRP: Kidney renal papillary cell carcinoma; MESO: Mesothelioma; UVM: Uveal melanoma; LAML: Acute myeloid leukemia; UCEC: Uterine corpus endometrial carcinoma; CESC: Cervical squamous cell carcinoma and endocervical adenocarcinoma; COAD: Colon adenocarcinoma; STAD: Stomach adenocarcinoma; LIHC: Liver hepatocellular carcinoma; THYM: Thymoma; BLCA: Bladder urothelial carcinoma; BRCA: Breast invasive carcinoma; LUSC: Lung squamous cell carcinoma; PCPG: Pheochromocytoma and paraganglioma; CHOL: Cholangiocarcinoma; HNSC: Head and neck squamous cell carcinoma; KICH: Kidney chromophobe; PRAD: Prostate adenocarcinoma; THCA: Thyroid carcinoma; UCS: Uterine carcinosarcoma.

paradoxical co-enrichment of cytotoxic ($CD8^+$ T cells, neutrophils) and suppressive (Tregs, M2 macrophages) populations, suggesting a dysfunctional immune activation phenotype. In contrast, LUAD and ACC displayed features of immune exclusion, with suppressed stromal and immune scores and depletion of multiple innate immune cell types. Interestingly, KIRC exhibited a unique myeloid-driven immunosuppressive architecture, with marked expansion of M0 macrophages and activated T cell subsets, accompanied by reduced dendritic and NK cell activity. These divergent immune profiles imply that exerkine-associated risk stratification encapsulates complex tumor–immune

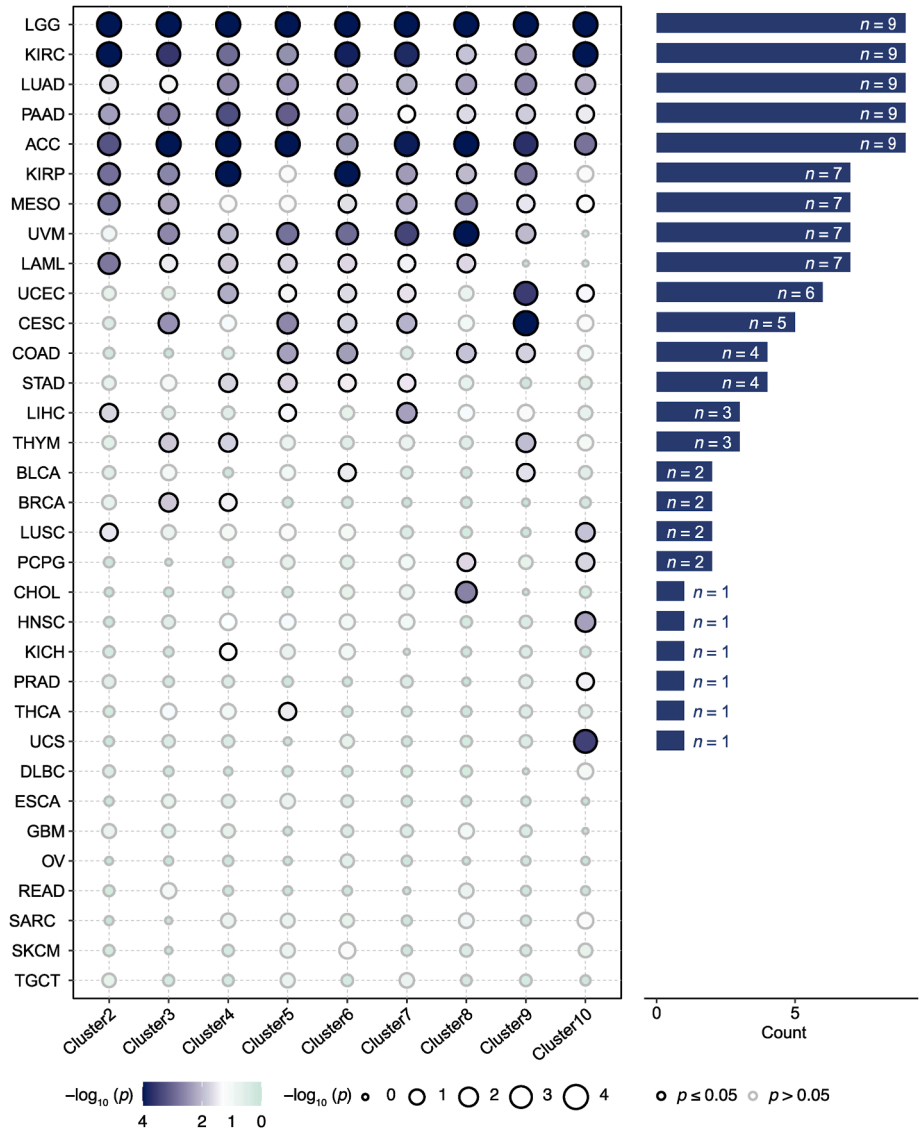

Fig. 3. Pan-cancer prognostic significance of NMF-derived exerkine clusters.
Left: Bubble plot illustrating log-rank p ($-\log_{10}$-transformed) for overall survival across all NMF cluster solutions ($k = 2$–10) in 33 cancers. Bubble size indicates effect magnitude; border color distinguishes significance (black = significant, gray = non-significant).
Right: Bar plot quantifying the number of cluster configurations per cancer with significant prognostic associations ($p < 0.05$).
LGG: Brain Lower Grade Glioma; KIRC: Kidney renal clear cell carcinoma; LUAD: Lung adenocarcinoma; PAAD: Pancreatic adenocarcinoma; ACC: Adrenocortical carcinoma; KIRP: Kidney renal papillary cell carcinoma; MESO: Mesothelioma; UVM: Uveal melanoma; LAML: Acute myeloid leukemia; UCEC: Uterine corpus endometrial carcinoma; CESC: Cervical squamous cell carcinoma and endocervical adenocarcinoma; COAD: Colon adenocarcinoma; STAD: Stomach adenocarcinoma; LIHC: Liver hepatocellular carcinoma; THYM: Thymoma; BLCA: Bladder urothelial carcinoma; BRCA: Breast invasive carcinoma; LUSC: Lung squamous cell carcinoma; PCPG: Pheochromocytoma and paraganglioma; CHOL: Cholangiocarcinoma; HNSC: Head and neck squamous cell carcinoma; KICH: Kidney chromophobe; PRAD: Prostate adenocarcinoma; THCA: Thyroid carcinoma; UCS: Uterine carcinosarcoma; DLBC: Diffuse large B - cell lymphoma; ESCA: Esophageal carcinoma;GBM: Glioblastoma multiforme; OV: Ovarian serous cystadenocarcinoma; READ: Rectum adenocarcinoma; SARC: Sarcoma; SKCM: Skin cutaneous melanoma; TGCT: Testicular germ cell tumors.

interactions that may influence both disease trajectory and therapeutic responsiveness.

Emerging literature further suggests that the secretion of specific exerkines is highly context-dependent, both in terms of tissue origin and exercise modality. For example, skeletal muscle–derived myokines such as FNDC5 (irisin), IL-6, and myostatin are predominantly induced by aerobic or endurance exercise, whereas resistance training preferentially promotes the release of IGF-1 and myostatin inhibitors. Adipose tissue contributes exerkines like adiponectin and leptin, while hepatokines such as FGF21 and ANGPTL4 are regulated by systemic metabolic cues. Importantly, the kinetics and magnitude of exerkine release vary with exercise intensity, with vigorous activity often eliciting more pronounced immunomodulatory responses. These modality- and tissue-specific secretion patterns suggest that the observed cancer-type–dependent exerkine clustering may reflect differences in how tumors interpret or respond to host-derived exercise signals. Therefore, personalized exercise prescriptions—accounting for tumor biology, exerkine sensitivity, and patient-specific physiology—could be key to optimizing therapeutic benefit in oncology.[6,9]

Checkpoint molecule expression further delineated the immunoregulatory heterogeneity across EPI strata. PD-L1 was significantly upregulated in high-EPI LUAD and ACC, while downregulated in KIRC, suggesting potential immune evasion pathways that differ across cancers. Similarly, CTLA4 expression increased only in high-risk KIRC and

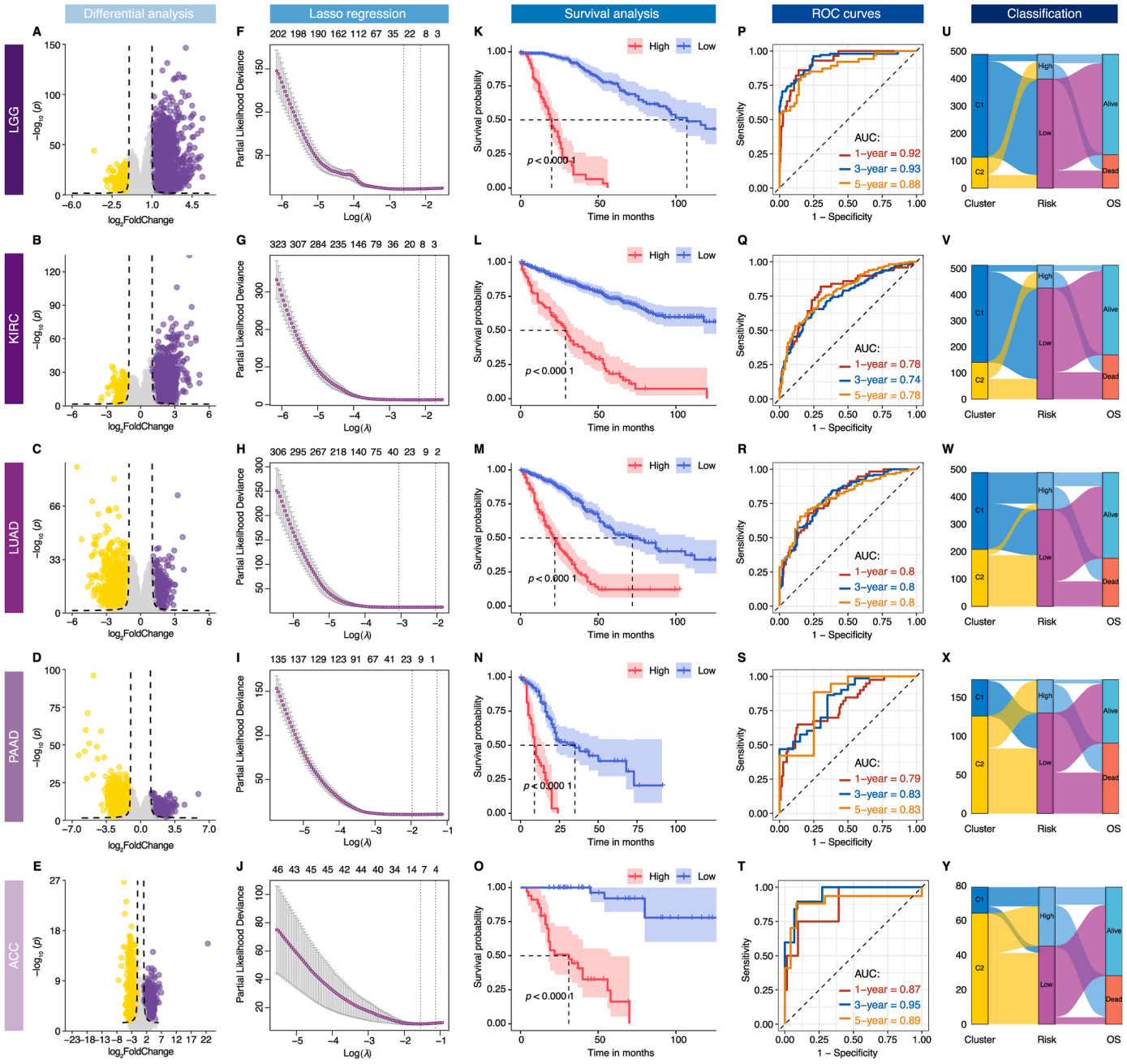

Fig. 4. Development and validation of the Exerkine Prognostic Index (EPI).
(A–E) Volcano plots of differentially expressed genes (DEGs) between NMF-derived clusters in LGG (Brain lower grade glioma), KIRC (Kidney renal clear cell carcinoma), LUAD (Lung adenocarcinoma), PAAD (Pancreatic adenocarcinoma), and ACC (Adrenocortical carcinoma) ($|\log_2(\text{FoldChange})| > 1$, $p < 0.05$).
(F–J) LASSO coefficient profiles derived from 10-fold cross-validation for EPI construction.
(K–O) Kaplan–Meier survival curves comparing high-vs. low-EPI subgroups (log-rank $p < 0.000\ 1$).
(P–T) Time-dependent ROC curves assessing EPI performance for 1-, 3-, and 5-year overall survival prediction.
(U–Y) Alluvial plots visualizing the concordance between NMF subtypes, EPI-defined risk groups, and clinical outcomes.

LUAD subgroups. These findings underscore the utility of EPI not only as a prognostic tool but also as a functional proxy for tumor immunogenicity, with implications for immunotherapy response prediction. Integrating exerkine-based classification with immune profiling could thus provide a more nuanced framework for stratifying patients in precision oncology.

Furthermore, our results lend credence to the hypothesis that exercise-induced molecular signals (exerkines) may differentially shape the tumor microenvironment and immune landscape depending on tumor type.[10,11] This reinforces the notion that exercise-based interventions may not yield uniform benefits across malignancies, but instead require cancer-specific optimization guided by molecular and immunological features.

The findings of this study also hold significant clinical implications. Risk stratification based on exerkines offers a new research direction for personalized cancer management and precision medicine. Identifying

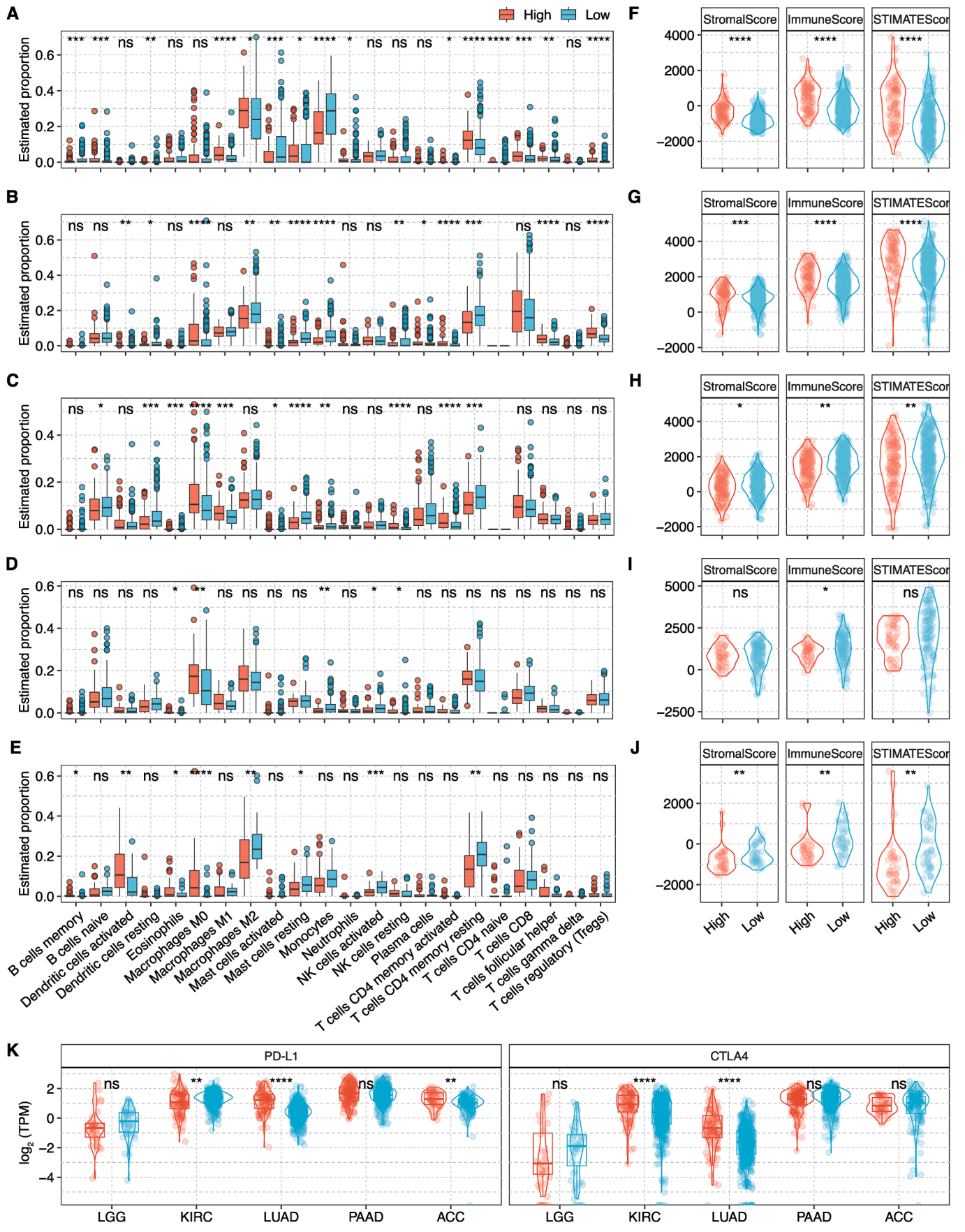

(caption on next page)

Fig. 5. Immune landscape and checkpoint dysregulation across EPI-defined risk groups.
(A–E) Boxplots comparing the relative abundance of 22 immune cell subsets (estimated via CIBERSORT, LM22 signature) between high- and low-EPI subgroups in LGG (Brain lower grade glioma), KIRC (Kidney renal clear cell carcinoma), LUAD (Lung adenocarcinoma), PAAD (Pancreatic adenocarcinoma), and ACC (Adrenocortical carcinoma).
(F–J) Violin plots showing StromalScore, ImmuneScore, and ESTIMATEScore differences (computed via the ESTIMATE algorithm) in LGG (Brain lower grade glioma), KIRC (Kidney renal clear cell carcinoma), LUAD (Lung adenocarcinoma), PAAD (Pancreatic adenocarcinoma), and ACC (Adrenocortical carcinoma).
(K)Differential expression of immune checkpoints (PD-L1 and CTLA4) between EPI subgroups. Statistical comparisons were performed using two-sided Mann–Whitney *U* tests. Significance levels: ns = not significant, $*p < 0.05$, $**p < 0.01$, $***p < 0.001$, $****p < 0.000\ 1$.

exerkine-related clusters associated with poor prognosis could provide valuable insights for clinicians to optimize comprehensive treatment plans. For instance, tailored exercise interventions based on tumor-specific characteristics might enhance therapeutic efficacy and improve patient survival outcomes.

4.1. Limitations

This study has several limitations. First, the exerkine gene set was derived from prior literature and may not fully encompass the dynamic and context-specific spectrum of exercise-responsive molecules. Second, the indirect inference of exercise effects through tumor-expressed exerkines does not fully capture the complexity of exercise–tumor interactions, particularly those mediated via systemic or non-transcriptional mechanisms. Third, although the EPI was validated across multiple cancer types using retrospective TCGA datasets, prospective validation in external cohorts and functional studies are necessary to confirm its clinical utility. Finally, the immune analyses were based on bulk transcriptomic deconvolution and lack spatial resolution; future single-cell and spatial transcriptomics studies are warranted to refine our understanding of exerkine-immune crosstalk in the tumor microenvironment.

5. Conclusions

In summary, this study presents a comprehensive, exerkine-driven framework for molecular classification and prognostic assessment across human cancers. By integrating NMF clustering, survival modeling, and immune microenvironment profiling, we demonstrate that exerkines stratify patients into clinically and biologically meaningful subgroups. The Exerkine Prognostic Index (EPI) accurately predicts overall survival and reveals distinct immune architectures and checkpoint dynamics in high-risk subgroups, offering potential avenues for immunotherapeutic refinement and personalized exercise-based interventions. These findings position exerkines as promising biomarkers at the intersection of metabolism, immunity, and cancer prognosis.

CRediT authorship contribution statement

Jiawei Du: Writing – original draft, Visualization, Methodology, Formal analysis, Data curation, Conceptualization. **Jinghua Hou:** Writing – review & editing, Supervision.

Data statement

All data used in our study are publicly available. RNA-seq data and corresponding clinical annotations for 33 cancer types were retrieved from the TCGA database via UCSC Xena (https://xena.ucsc.edu/).

Funding

This study was supported by Beijing Sport University Graduate Innovation Programme (2024013).

Declaration of competing interest

The authors declare that they have no competing interests.

Appendix A. Supplementary data

Supplementary data to this article can be found online at https://doi.org/10.1016/j.smhs.2025.05.002.

References

1. Ligibel JA, Bohlke K, May AM, et al. Exercise, diet, and weight management during cancer treatment: ASCO guideline. *J Clin Oncol*. 2022;40(22):2491–2507. https://doi.org/10.1200/jco.22.00687.
2. Campbell KL, Winters-Stone KM, Wiskemann J, et al. Exercise guidelines for cancer survivors: consensus statement from international multidisciplinary roundtable. *Med Sci Sports Exerc*. 2019;51(11):2375–2390. https://doi.org/10.1249/mss.0000000000002116.
3. Rock CL, Thomson CA, Sullivan KR, et al. American Cancer Society nutrition and physical activity guideline for cancer survivors. *CA Cancer J Clin*. 2022;72(3):230–262. https://doi.org/10.3322/caac.21719.
4. Hojman P, Gehl J, Christensen JF, Pedersen BK. Molecular mechanisms linking exercise to cancer prevention and treatment. *Cell Metab*. 2018;27(1):10–21. https://doi.org/10.1016/j.cmet.2017.09.015.
5. Courneya KS, Booth CM. Exercise as cancer treatment: a clinical oncology framework for exercise oncology research. *Front Oncol*. 2022;12:957135. https://doi.org/10.3389/fonc.2022.957135.
6. Orange ST, Leslie J, Ross M, Mann DA, Wackerhage H. The exercise IL-6 enigma in cancer. *Trends Endocrinol Metab*. 2023;34(11):749–763. https://doi.org/10.1016/j.tem.2023.08.001.
7. Chow LS, Gerszten RE, Taylor JM, et al. Exerkines in health, resilience and disease. *Nat Rev Endocrinol*. 2022;18(5):273–289. https://doi.org/10.1038/s41574-022-00641-2.
8. Nagaraju GP, Sharma D. Anti-cancer role of SPARC, an inhibitor of adipogenesis. *Cancer Treat Rev*. 2011;37(7):559–566. https://doi.org/10.1016/j.ctrv.2010.12.001.
9. Jia N, Zhou Y, Dong X, Ding M. The antitumor mechanisms of aerobic exercise: a review of recent preclinical studies. *Cancer Med*. 2021;10(18):6365–6373. https://doi.org/10.1002/cam4.4169.
10. Koelwyn GJ, Quail DF, Zhang X, White RM, Jones LW. Exercise-dependent regulation of the tumour microenvironment. *Nat Rev Cancer*. 2017;17(10):620–632. https://doi.org/10.1038/nrc.2017.78.
11. Koelwyn GJ, Zhuang X, Tammela T, Schietinger A, Jones LW. Exercise and immunometabolic regulation in cancer. *Nat Metab*. 2020;2(9):849–857. https://doi.org/10.1038/s42255-020-00277-4.

Jiawei Du[a,b,1], Jinghua Hou[a,c,*,1]
[a] *Key Laboratory of Sports and Physical Fitness of the Ministry of Education, Beijing Sport University, Beijing, China*
[b] *Department of Exercise Physiology, Beijing Sport University, Beijing, China*
[c] *Department of Exercise biochemistry, Beijing Sport University, Beijing, China*

[*] Corresponding author. Department of Exercise Biochemistry, Beijing Sport University, Beijing, China.
E-mail address: houjh@bsu.edu.cn (J. Hou).

[1] These authors contributed equally to this work.